nature communications

Article

https://doi.org/10.1038/s41467-023-41298-3

2-Oxabicyclo[2.2.2]octane as a new bioisostere of the phenyl ring

Received: 13 January 2023

Accepted: 30 August 2023

Published online: 02 October 2023

Check for updates

Vadym V. Levterov[1], Yaroslav Panasiuk[1], Kateryna Sahun[1], Oleksandr Stashkevych[1], Valentyn Badlo[1], Oleh Shablykin[1,2], Iryna Sadkova[1], Lina Bortnichuk[1], Oleksii Klymenko-Ulianov[1], Yuliia Holota[1], Leonid Lachmann[3], Petro Borysko[1], Kateryna Horbatok[1], Iryna Bodenchuk[1], Yuliia Bas[4], Dmytro Dudenko[1] & Pavel K. Mykhailiuk[1]

The phenyl ring is a basic structural element in chemistry. Here, we show the design, synthesis, and validation of its new saturated bioisostere with improved physicochemical properties – 2-oxabicyclo[2.2.2]octane. The design of the structure is based on the analysis of the advantages and disadvantages of the previously used bioisosteres: bicyclo[1.1.1]pentane, bicyclo[2.2.2]octane, and cubane. The key synthesis step is the iodocyclization of cyclohexane-containing alkenyl alcohols with molecular iodine in acetonitrile. 2-Oxabicyclo[2.2.2]octane core is incorporated into the structure of Imatinib and Vorinostat (SAHA) drugs instead of the phenyl ring. In Imatinib, such replacement leads to improvement of physicochemical properties: increased water solubility, enhanced metabolic stability, and reduced lipophilicity. In Vorinostat, such replacement results in a new bioactive analog of the drug. This study enhances the repertoire of available saturated bioisosteres of (hetero)aromatic rings for the use in drug discovery projects.

The phenyl ring is a basic structural element in chemistry. It is one of the most common structural motifs in natural products[1] and bioactive compounds[2,3]. Moreover, more than five hundred drugs contain a fragment of *para*-substituted phenyl ring (Fig. 1a, b)[4], including the well-known to everyone Paracetamol. However, organic compounds with more than two phenyl rings often suffer from poor solubility[5–7].

In 2012, however, Stepan and colleagues showed that a replacement of the central phenyl ring in a γ-secretase inhibitor with the bicyclo[1.1.1]pentane improved its physicochemical properties and retained bioactivity[8–11]. Later, analogous replacements were undertaken with cubane[12–19], and bicyclo[2.2.2]octane (Fig. 1a, b)[20–22]. Therefore, during the past decade, these scaffolds proved to be useful in drug discovery, medicinal chemistry, and supramolecular chemistry[23–31]. Replacement of the *ortho*- and *meta*-substituted phenyl rings in bioactive compounds with saturated bioisosteres was also recently achieved[26–31]. Recent studies, however, showed that all three bioisosteres had drawbacks. In bicyclo[1.1.1]pentane, the most popular among them today[32–40], the distance between two bridgehead carbon atoms (C-C) is 1.8 Å, which is ca. 35% shorter than that in the *para*-substituted phenyl ring (2.8 Å). Bicyclo[2.2.2]octane has a closer C-C distance (2.6 Å), but higher lipophilicity[41]. Cubane, in turn, was recently demonstrated to be unstable under contact with transition metals[42,43], under mechanochemical treatment or heating[44].

In this work, we have rationally designed, synthesized, and characterized the new bioisostere of the phenyl ring – 2-oxabicyclo[2.2.2]octane (Fig. 1c).

Interestingly, 2-oxabicyclo[2.2.2]octane core has been known in the literature, but not in the context of phenyl bioisostere. Chemists used it as a starting material in organic synthesis;[45,46] and in medicinal chemistry[47–49] as an analog of 4-aminopiperidine[50–53] or cyclohexane[54,55]. Also, 2-oxabicyclo[2.2.2]octane containing molecules exhibited a broad range of biological activities: estrogen receptor-beta

[1]Enamine Ltd., Winston Churchill street 78, 02094 Kyiv, Ukraine. [2]V. P. Kukhar IBOPC of the NASciences of Ukraine, Academician Kukhar Str. 1, 02094 Kyiv, Ukraine. [3]Bienta, Winston Churchill street 78, 02094 Kyiv, Ukraine. [4]Taras Shevchenko National University of Kyiv, Chemistry Department, Volodymyrska 64, 01601 Kyiv, Ukraine. e-mail: Pavel.Mykhailiuk@gmail.com

https://doi.org/10.1038/s41467-023-41298-3

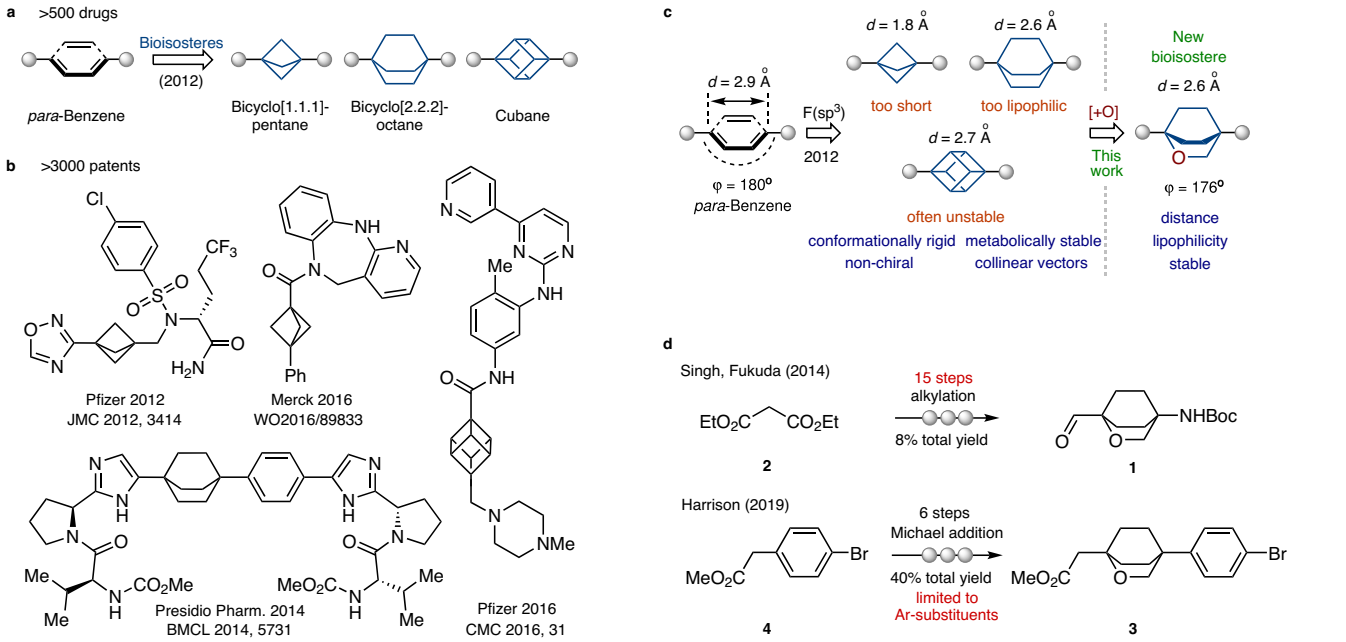

Fig. 1 | The *para*-substituted phenyl ring and its saturated bioisosteres. a The *para*-substituted phenyl ring is a part of >500 drugs and agrochemicals. Bicyclo[1.1.1]pentanes, bicyclo[2.2.2]octanes, and cubane as saturated bioisosteres of the *para*-substituted phenyl ring. **b** Bioactive derivatives of bicyclo[1.1.1]pentanes, bicyclo[2.2.2]octanes, and cubane are described in >3000 patents. **c** Aim of this work: replacement of the *para*-substituted phenyl ring in bioactive compounds with 2-oxabicyclo[2.2.2]heptane. **d** Previous syntheses of 2-oxabicyclo[2.2.2]heptane by Singh, Fukuda (2014)[50] and Harrison (2019)[54].

agonists[47], myeloperoxidase inhibitors[48], antibacterial agents[49–53], DGAT1 Inhibitors[54], and RORγt agonists[55].

Results

Design

In the design of the improved phenyl bioisostere, we first needed to keep the advantages of the previously used cores: their conformational rigidity, metabolic stability, non-chirality, and collinearity of vectors ($\varphi = 180°$). At the same time, we needed to address their drawbacks: C-C distance, and lipophilicity. Considering the possible saturated structures (for the details of the design, please, see Supplementary Iinformation, page 5, Supplementary Fig. 1.), we decided to select the bicyclo[2.2.2]octane scaffold, because of its appropriate C-C distance, and decorate it with an oxygen atom. In particular, replacing one carbon atom with oxygen would give 2-oxabicyclo[2.2.2]octane with similar geometry and reduced lipophilicity (Fig. 1c). Also, this structure should be chemically stable as a simple derivative of tetrahydropyran.

Optimization

Synthesis of the 2-oxabicyclo[2.2.2]octane core has been previously reported. In 2014, Singh and Fukuda obtained compound **1** from diethyl malonate (**2**) in 15 steps using alkylation as a key reaction (Fig. 1d)[50]. In 2019, Harrison synthesized compound **3** from ester **4** in six steps employing an intramolecular Michael addition (Fig. 1d)[54]. The latter approach was limited only to aromatic substituents. We, however, needed a general modular method that would give 2-oxabicyclo[2.2.2]octanes with one or two functional groups that could be subsequently modified to obtain a wide variety of derivatives - bioisosteres of the *mono*- and *para*-substituted phenyl rings.

Previously, we showed that smaller 2-oxabicyclo[2.1.1]hexane could be assembled via the iodocyclization reaction of the corresponding cyclobutane alkenyl alcohols[56]. The reaction proceeded with I_2/$NaHCO_3$ in the mixture of water and MeO*t*Bu at room temperature. We hoped that similar cyclization would also take place with cyclohexane **5** (please, see its preparation below). However, under analogous conditions the expected product **6** was not formed (Table 1, entry 1). We repeated the reaction several times varying the time and the temperature, however, with the same negative outcome (Table 1, entries 2-4). The addition of the iodine molecule to the double C=C bond did take place, but the cyclization failed to occur.

Subsequently, we realized that in contrast to the already conformationally preorganized small cyclobutane, the larger and more flexible cyclohexane ring should adopt the highly energetic boat

Table 1 | Optimization of the synthesis of compound 6

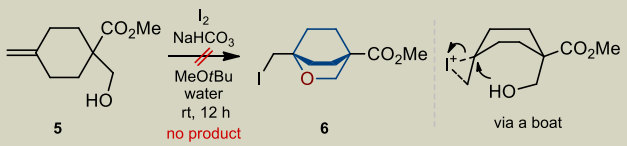

Entry	Conditions	Yield (%)[a]
1	I_2, $NaHCO_3$, MeO*t*Bu, H_2O, rt, 12 h	n.d.
2	I_2, $NaHCO_3$, MeO*t*Bu, H_2O, rt, 48 h	n.d.
3	I_2, $NaHCO_3$, MeO*t*Bu, H_2O, rt, 1 h	n.d.
4	I_2, $NaHCO_3$, MeO*t*Bu, H_2O, reflux, 12 h	n.d.
5	I_2, $NaHCO_3$, Et_2O, H_2O, rt, 12 h	n.d.
6	I_2, $NaHCO_3$, dioxane, H_2O, rt, 12 h	n.d.
7	I_2, $NaHCO_3$, dioxane, rt, 12 h	n.d.
8	I_2, $NaHCO_3$, MeO*t*Bu, rt, 12 h	n.d.
9	I_2, $NaHCO_3$, DMF, rt, 12 h	<10
10	I_2, $NaHCO_3$, DMSO, rt, 12 h	<10
11	I_2, $NaHCO_3$, NMP, rt, 12 h	<10
12	I_2, $NaHCO_3$, CH_3CN, rt, 12 h	56
13	I_2, $NaHCO_3$, CH_3CN, reflux, 12 h	45
14	Br_2, $NaHCO_3$, CH_3CN, rt, 12 h	30

N.d. not determined.
[a]Isolated yield.

https://doi.org/10.1038/s41467-023-41298-3

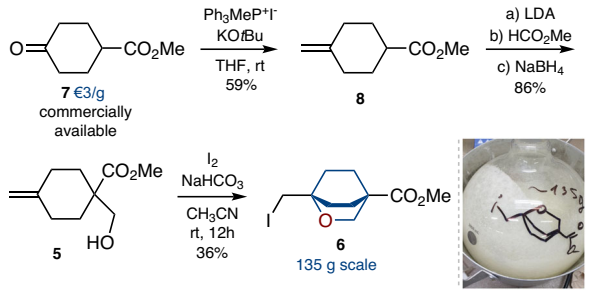

Fig. 2 | Scalable synthesis of 2-oxabicyclo[2.2.2]octane 6. The synthesis started from the commercially available ketone **7**. Iodide **6** was obtained on a 135 g scale in one run.

conformation first (Table 1). The resulting entropic penalty seems to prevent the cyclization from occuring. We also tried other combinations of solvents with no success, however (Table 1, entries 5-8). Finally, we used solely dipolar aprotic solvents. Indeed, in dimethyl formamide, the formation of traces of the needed product was finally seen (Table 1, entry 9). A similar result was observed in dimethyl sulfoxide and *N*-methyl pyrrolidone (Table 1, entries 10, 11). In acetonitrile, the transformation proceeded cleaner, and iodide **6** was obtained in a 56% yield (Table 1, entry 12). Performing the reaction under heating (Table 1, entry 13) or employing bromine (Br_2; Table 1, entry 14) did not improve the yield.

Scalable synthesis

Having a working procedure in hand, we studied its scalability. The whole synthesis scheme commenced from the commercially available ketoester **7** (ca. 3€/g, Fig. 2). Wittig reaction gave alkene **8** in 59% yield. Treatment of the latter with LDA/methyl formate followed by the reduction of the intermediate aldehyde with $NaBH_4$ gave alcohol **5** in 86% combined yield. Finally, the key iodocyclization was attempted on a multigram scale. Pure iodide **6** was obtained as a white crystalline solid after column chromatography with a 36% yield. Despite a rather moderate yield, this protocol allowed us to obtain 135 g of the product in a single run.

Scope

Next, we studied the generality of the developed protocol. Treatment of alkene **8** with LDA/acetaldehyde gave the intermediate alcohol that was used in the subsequent iodocyclization under the developed conditions. The expected iodide **9** was isolated in 50% yield after column chromatography (Fig. 3a). Initially, we isolated the intermediate alcohol, but subsequently, we understood that performing the two-step procedure with a simple solvent swap ensured a better yield of the final product.

The reaction with aliphatic (**10**–**12**), aromatic (**13**–**17**), and heterocyclic (**18**–**27**) aldehydes gave the corresponding 2-oxabicyclo[2.2.2]octanes in good yields. Functional groups such as nitro, trifluoromethoxy, trifluoromethyl, nitrile, and halogen atoms tolerated the reaction conditions. The protocol was not without limitations, however. We could not obtain products **28**, and **29** with thiazole and triazole heterocycles, due to the formation of complex mixtures (Fig. 3a). Ketones could also be used as electrophiles instead of aldehydes. As a representative example, the reaction of alkene **8** with LDA/acetone followed by iodocyclization gave dimethyl-substituted product **30** in 81% yield. The structure of **30** was confirmed by X-ray crystallographic analysis (Fig. 3b, Supplementary Data 1). A reduction of **8** followed by iodocyclization gave iodide **31** in 58% yield. Interestingly, the cyclization was not efficient at room temperature, and required heating. Alkylation of **8** with MeI or $BnOCH_2Cl$ followed by reduction and iodocyclization gave the disubstituted products **32, 33** in 59-64% yield (Fig. 3b).

Trisubstituted exocyclic alkenes also afforded the desired 2-oxabicyclo[2.2.2]octane skeleton. For example, the iodocyclization of alkene **34** under the standard conditions gave iodide **35** in 67% yield (Fig. 3c). Alkene **36** provided iodide **37** in 50% yield. Endocyclic alkene **38**, however, gave the isomeric core - 6-oxabicyclo[3.2.1]octane **39**[57].

We also tried to assemble a 2-azabicyclo[2.2.2]octane skeleton using the developed strategy. An attempted iodocyclization of alkene **40** did not lead to the formation of the cyclic iodide **41** neither at room temperature nor under heating (Fig. 3d). However, the analogous reaction of the bridgehead-substituted alkene **42** at room temperature did give the needed product **43** in 31% yield. Under heating, the yield was improved to 41%.

Modifications

Several representative modifications of the obtained iodides were undertaken to obtain various *mono*- and bifunctional 2-oxabicyclo[2.2.2]octanes ready for direct use in medicinal chemistry projects. Treatment of iodide **31** with potassium thioacetate followed by oxidation with NCS gave aliphatic sulfonyl chloride **44** in 85% yield. The reaction of **31** with potassium acetate and the subsequent alkali hydrolysis provided valuable alcohol **45**. Oxidation of the latter afforded carboxylic acid **46** in 89% yield (Fig. 4).

Hydrogenative reduction of the C-I bond in iodide **6** followed by saponification of the ester group gave methyl acid **47**. The Curtius reaction of the latter resulted in amine **48**. The reaction of iodide **6** with $LiAlH_4$ gave alcohol **49** in 90% yield. O-Mesylation and the subsequent reaction with LiBr provided bromide **50**. Swern oxidation of alcohol **49** gave aldehyde **51** in 63% yield. Isomeric methyl-substituted 2-oxabicyclo[2.2.2]octanes were obtained from iodide **32**. Its reaction with sodium azide followed by the reduction formed amine **52**. The reaction of iodide **32** with potassium acetate and hydrolysis gave alcohol **53** - isomer of alcohol **49**. Oxidation of **53** formed carboxylic acid **54** - isomer of acid **47**. Sulfonyl chloride **55** was also obtained from iodide **32** via a two-step procedure (Fig. 4).

From iodide **6** we also synthesized various bifunctional linkers for incorporation into bioactive compounds instead of the *para*-substituted phenyl ring. Saponification of ester **6** provided carboxylic acid **56** in 90% yield. The subsequent Curtius reaction afforded *N*-Boc iodide **57** in 87% yield. The structure of **57** was confirmed by X-ray crystallographic analysis (Supplementary Data 2). The reaction of the latter with potassium acetate, followed by ester hydrolysis (via **58**) and *N*-Boc acidic deprotection gave amino alcohol **59**. Oxidation of the alcohol group in **58** gave *N*-Boc protected amino acid **60** – a saturated analog of the *para*-aminobenzoic acid. The reaction of iodide **57** with NaN_3 (via azide **61**) followed by reduction of the azide group formed diamine **62**. The reaction of iodide **6** with NaN_3 (via azide **63**), the subsequent reduction (via **64**), N-Boc protection, and saponification gave another *N*-Boc protected amino acid **65**. The Curtius reaction of the latter provided *N*-Boc diamine **66** – isomer of diamine **62**. The reaction of iodide **6** with sodium azide followed by extensive reduction of the intermediate azide with $LiAlH_4$ gave amino alcohol **67**. The structure of **67** was confirmed by X-ray crystallographic analysis (Supplementary Data 3). The reaction of iodide **6** with potassium acetate (via **68**) followed by saponification of the ester group and oxidation gave linker **69**. Its structure was also confirmed by X-ray crystallographic analysis (Supplementary Data 4). Worth noting that all the above-described syntheses depicted in Fig. 4 were realized on a multigram scale.

Alkylation of 4-bromothiophenol with iodide **32** followed by oxidation of the intermediate sulfide gave sulfone **70** in 54% yield over two steps (Fig. 4). Sulfonamide **71** was obtained in 44% yield from amine **48**. Cu-catalyzed click reaction between azide **63** and 3-ethynylquinoline smoothly provided triazole **72**. Condensation of acid **73** with *N*-hydroxyphthalimide (NHPI) in the presence of N,N′-diisopropylcarbodiimide (DIC) gave the activated ester **74** (Fig. 4). Ni-mediated

https://doi.org/10.1038/s41467-023-41298-3

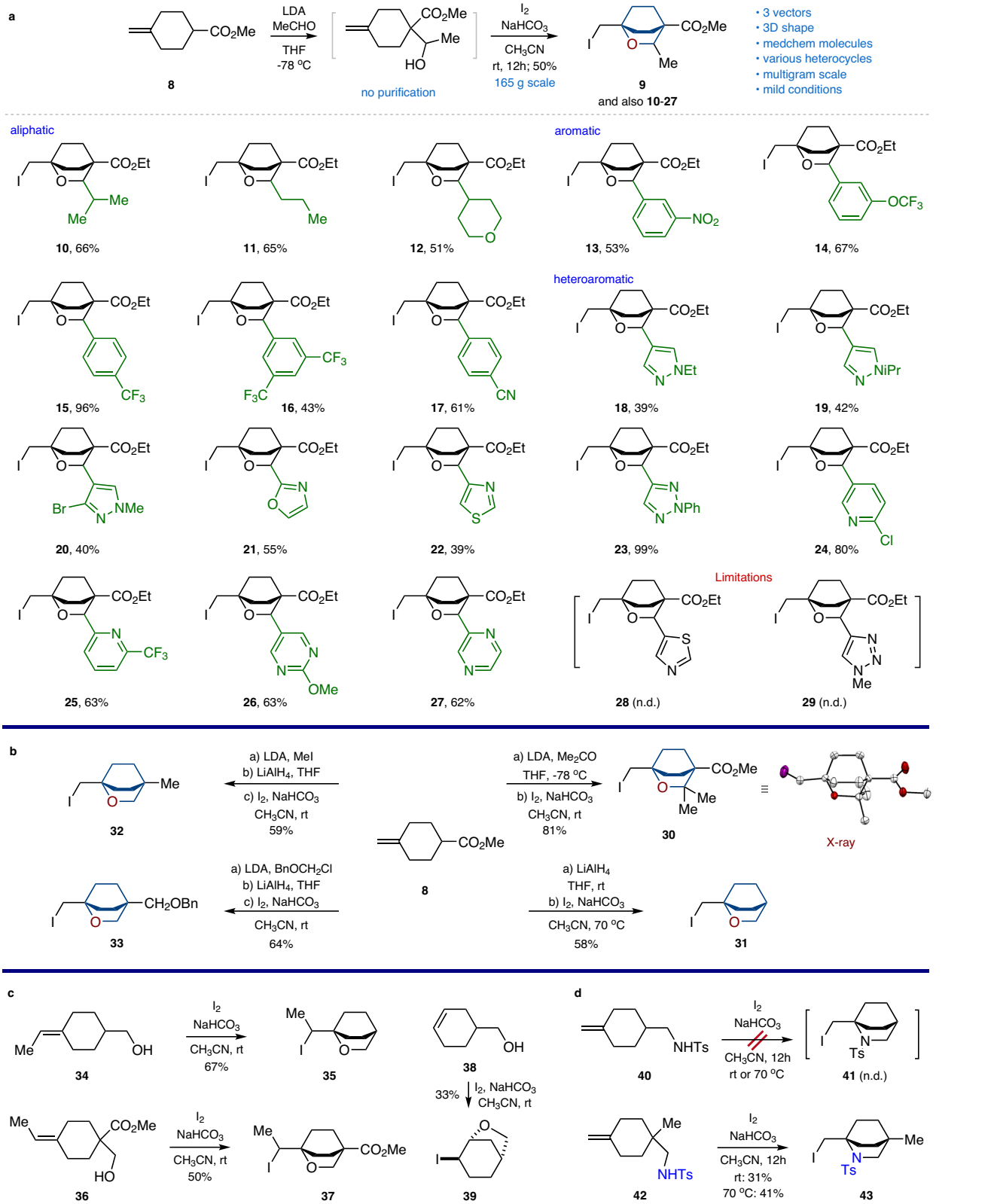

Fig. 3 | Synthesis of 2-oxabicyclo[2.2.2]octanes and 2-azabicyclo[2.2.2]octanes. **a** Synthesis of 2-oxabicyclo[2.2.2]octanes with three exit vectors (for products **10**–**29**, ethyl ester analog of alkene **8** was used). **b** Synthesis of 2-oxabicyclo[2.2.2] octanes with one and two exit vectors. X-ray crystal structure of compound **30b** (carbon – white, oxygen – red, iodine - violet). Hydrogen atoms are omitted for clarity. **c** Iodocyclization of alkenes **34, 36**, and **38**. **d**, Synthesis of 2-azabicyclo[2.2.2]octane **43**.

https://doi.org/10.1038/s41467-023-41298-3

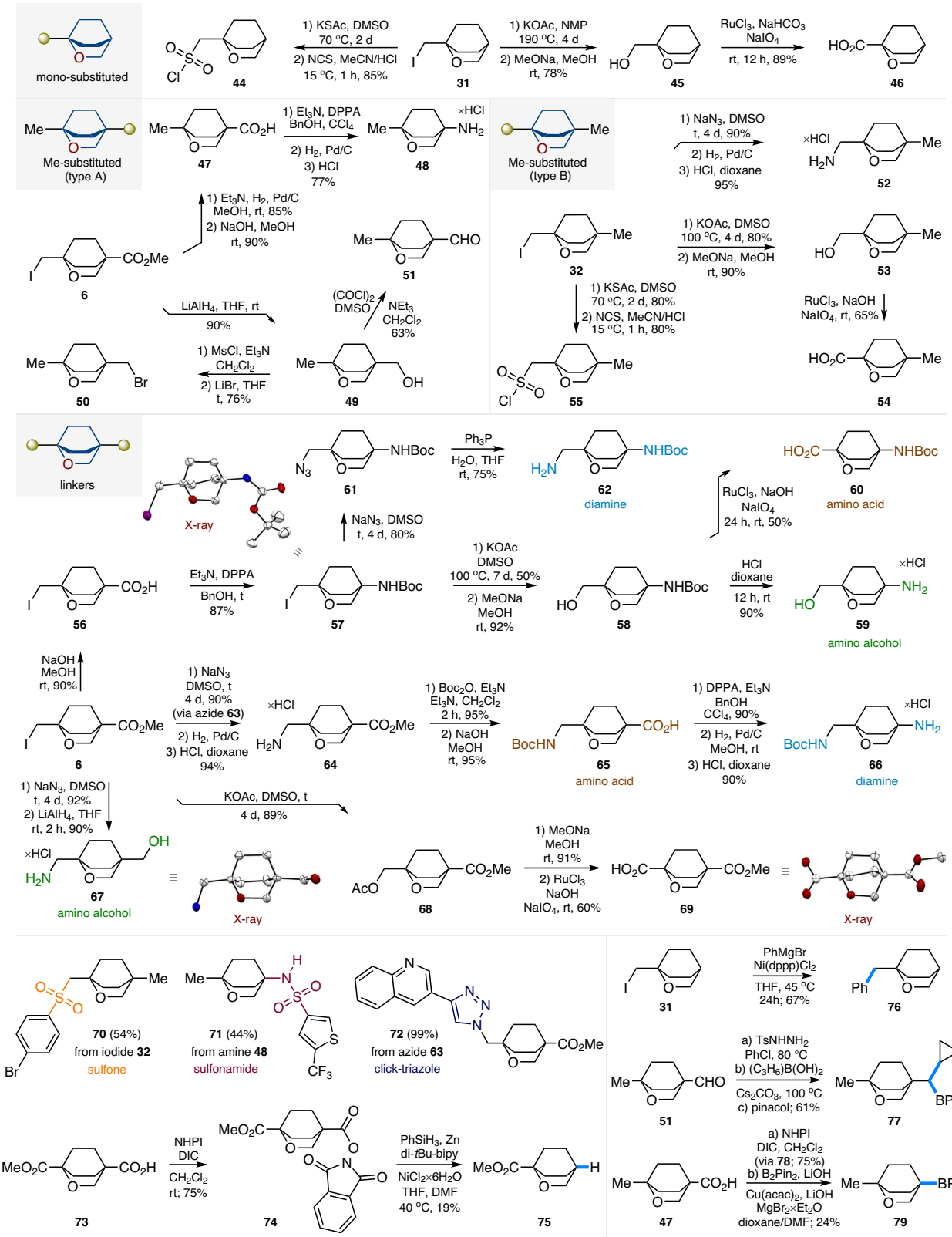

Fig. 4 | Synthesis of functionalized 2-oxabicyclo[2.2.2]octanes for medicinal chemistry. X-ray crystal structure of compounds **57, 67**, and **69** (carbon – white, oxygen – red, nitrogen – blue, iodine - violet). Hydrogen and chlorine atoms are omitted for clarity.

Barton decarboxylation[58] of the latter with $PhSiH_3$ was performed next to provide ester **75**.

Ni-Mediated C-C cross-coupling of iodide **31** with PhMgBr gave 2-oxabicyclo[2.2.2]octane **76** in 67% yield. The reaction of aldehyde **51** with p-toluenesulfonyl hydrazide gave the intermediate hydrazone that upon treatment with the cyclopropylboronic acid and pinacol provided organoboron derivative **77**[59]. Condensation of acid **47** with *N*-hydroxyphthalimide gave the activated ester **78**. Its structure was confirmed by X-ray crystallographic analysis (Supplementary Data 5). Cu-Catalyzed

https://doi.org/10.1038/s41467-023-41298-3

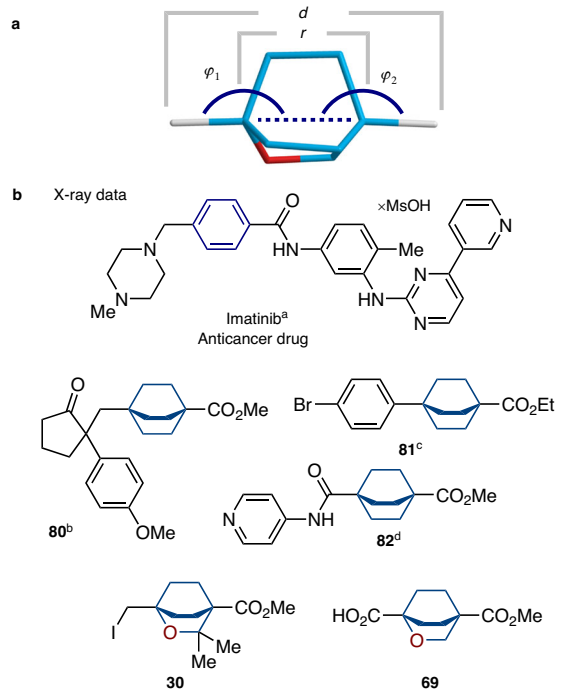

Compound	r (Å)	d (Å)	φ_1 (°)	φ_2 (°)
Imatinib (A)	2.893(0)	5.925(0)	176.4(8)	178.5(9)
Imatinib (B)	2.883(2)	5.906(0)	176.7(3)	178.7(5)
80	2.606(6)	5.62(1)	175.3(2)	177.1(2)
81	2.624(2)	5.656(2)	177.2(1)	177.0(1)
82	2.615(2)	5.665(2)	178.8(6)	178.7(1)
30	2.555(5)	5.582(5)	174.5(2)	177.3(2)
69	2.539(3)	5.563(3)	176.0(5)	176.4(1)

Fig. 5 | Crystallographic analysis of 2-oxabicyclo[2.2.2]octanes. a Definition of distances *r*, *d* and angles φ_1, φ_2 (2-oxabicyclo[2.2.2]octane core is shown as example). **b** Geometric parameters *r*, *d* and φ_1, φ_2 for *para*-substituted phenyl ring (Imatinib drug), its known saturated bioisosteres **80**–**82** and the new saturated bioisosteres **30, 69**. aData is taken from ref. 64. bData is taken from ref. 61. cData is taken from ref. 62. dData is taken from ref. 63. Two individual molecules of Imatinib (A and B) are present in the crystal lattice.

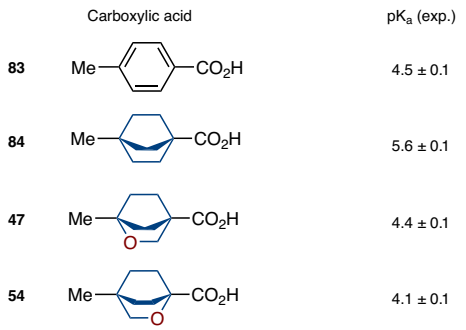

Fig. 6 | Experimental pKa values of carboxylic acids 47, 54, 83, and 84. Data is obtained by the titration method. *Para*-methyl benzoic acid (**83**) is used as a reference.

decarboxylative borylation[60] of ester **78** gave organoboron derivative **79** (Fig. 4).

Chemical stability

We also examined the thermal and chemical stability of the synthesized 2-oxabicyclo[2.2.2]octanes. As representative examples, we selected three molecules: isomeric acids **47, 54**, and amine **52**. All 2-oxabicyclo[2.2.2]octanes were crystalline solids that were stable in air. We stored them in stock at room temperature in closed vials and observed no changes according to ^{1}H NMR after one year. Also, the compounds remained stable even under heating at 100 °C for five minutes. Treatment of the selected 2-oxabicyclo[2.2.2]octanes with aq. 1 M HCl, or aq. 1 M NaOH at room temperature for 1 h resulted in no decomposition either.

Crystallographic analysis

Next, we compared the geometric properties of 2-oxabicyclo[2.2.2]octanes with those of the *para*-substituted phenyl ring, and the previously used bioisosteres - bicyclo[2.2.2]octanes. For this purpose, we measured two C-C distances *r* and *d* to see the overall similarity of cores; and two angles φ_1 and φ_2 to estimate the collinearity of exit vectors (Fig. 5a).

We calculated the values of *r*, *d*, φ_1, and φ_2 of 2-oxabicyclo[2.2.2]octanes from the X-ray data of compounds **30, 69**. The related parameters for bicyclo[2.2.2]octanes **80**[61], **81**[62], and **82**[63] were calculated from their X-ray data published in the literature (Fig. 5b). The corresponding parameters for the *para*-substituted phenyl ring were calculated from the reported crystal structure of the anticancer drug Imatinib[64]. Analysis of this data revealed that the geometric properties of 2-oxabicyclo[2.2.2]octanes were indeed very similar to those of the *para*-substituted phenyl ring. The distance r in 2-oxabicyclo[2.2.2]octanes was ca. 0.3 Å shorter than that in the *para*-phenyl ring: 2.54–2.56 Å vs 2.88–2.89 Å (*para*-phenyl). The distance d between substituents in 2-oxabicyclo[2.2.2]octanes was also ca. 0.3 Å shorter than that in the *para*-phenyl ring: 5.56–5.58 Å vs 5.90–5.93 Å (*para*-phenyl). The difference in collinearity of vectors was insignificant, as angles φ_1 and φ_2 were almost identical in both scaffolds: 176-177° vs 178-179° (*para*-phenyl). Interestingly, even in the *para*-substituted phenyl ring in Imatinib in the crystal phase, the observed angles φ_1 and φ_2 deviated from the ideal value of 180°: 176-179°. It must be noted, that all parameters, - *r*, *d*, φ_1 and φ_2, - were also almost identical in both bicyclo[2.2.2]octanes (**80**–**82**) and 2-oxabicyclo[2.2.2]octanes (**30, 69**) (Fig. 5b).

In short summary, the replacement of the methylene group for an oxygen atom in the bicyclo[2.2.2]octane core did not affect its three-dimensional geometry. Moreover, the formed 2-oxabicyclo[2.2.2]octane core resembled well the *para*-substituted phenyl ring, as the geometric parameters r, d, φ_1, and φ_2 remained very similar (please, see SI, page 277, Supplementary Fig. 8).

The acidity of functional groups

We also studied the influence of the replacement of the methylene group for an oxygen atom in the bicyclo[2.2.2]octane skeleton on the electronic properties. Towards this goal, we measured experimental pK_a values of isomeric 2-oxabicyclo[2.2.2]octane carboxylic acids **47** and **54**, bicyclo[2.2.2]octane carboxylic acid **84**, and *para*-methyl benzoic acid (**83**) as a reference (Fig. 6). Replacement of the methylene group in **84** for the oxygen atom at the distal γ-position notably increased its acidity from $pK_a = 5.6$ to 4.4 (**47**). However, analogous replacement at the β-position increased the acidity even more to $pK_a = 4.1$ (**54**).

Important to mention that the acidity of aromatic carboxylic acid **83** and 2-oxabicyclo[2.2.2]octane **47** were almost identical (Fig. 6). The replacement of the phenyl ring in acid **83** with the bicyclo[2.2.2]octane core reduced the acidity: $pK_a = 4.5$ (**83**) vs 5.6 (**84**). However, incorporation of the β-oxygen atom into the latter ideally restored it: $pK_a = 4.4$ (**47**). Because the acidity/basicity of functional groups is often responsible for the potency, selectivity, and toxicity of bioactive compounds[65], the fine-tuning of the pK_a by replacing the phenyl ring with isomeric 2-oxabicyclo[2.2.2]octanes could become a preferred solution.

https://doi.org/10.1038/s41467-023-41298-3

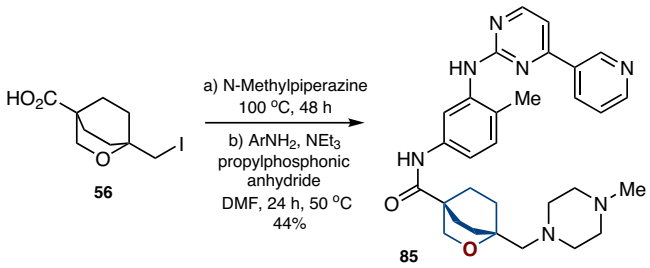

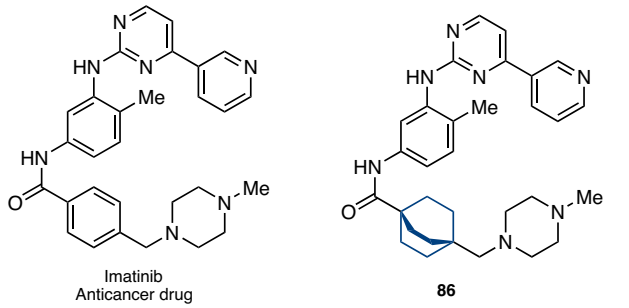

Compound	Solubility	clogP	logD (7.4)	CL_{int}	$t_{1/2}$
Imatinib	351±2	4.5	2.6±0.1	28	60
86	113±1	3.6	2.7±0.1	16	107
85	389±1	2.6	1.8±0.1	19	87

Fig. 7 | Replacement of the *para*-phenyl ring with saturated bioisosteres in anticancer drug Imatinib. Solubility: experimental kinetic solubility in phosphate-buffered saline, pH 7.4 (μM). clogP: calculated lipophilicity. logD (7.4): experimental distribution coefficient in *n*-octanol/phosphate-buffered saline, pH 7.4. Reliable logD measured were obtained within a range of 1.0–4.5. CL_{int} clearance intrinsic: experimental metabolic stability in human liver microsomes (μl/min/mg). $t_{1/2}$ (min) experimental half-time of a metabolic decomposition.

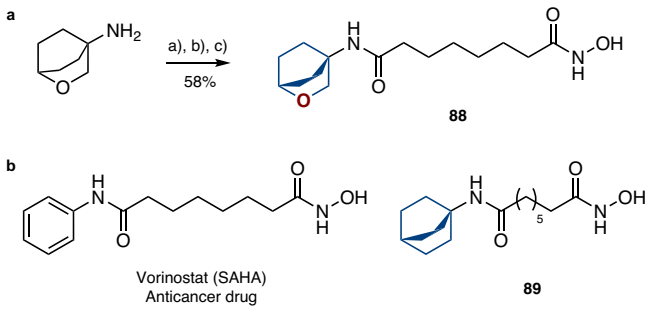

Fig. 8 | Replacement of the phenyl ring with saturated bioisosteres in anticancer drug Vorinostat (SAHA). a Synthesis of compound **88** – a saturated analog of Vorinostat. Reaction conditions: a) $Cl(O)C(CH_2)_6CO_2Me$, NEt_3, CH_2Cl_2, rt, 2 h. b) NaOH, MeOH, reflux, 30 min. c) NH_2OH•HCl, DMF, CDI, rt, 30 min. **b** Structure of Vorinostat (SAHA), and its saturated analog **89**.

Incorporation into drugs

To demonstrate the practical utility of the 2-oxabicyclo[2.2.2]octane scaffold, we incorporated it into the structure of anticancer drugs Imatinib, and Vorinostat (SAHA) instead of the *para*- and *mono*-substituted phenyl rings, correspondingly (Figs. 7 and 8).

The reaction of iodide **56** with *N*-methyl piperazine, followed by acylation with the substituted aniline gave compound **85** – a saturated analog of Imatinib (Fig. 7). For comparison, we also synthesized compound **86** with the bicyclo[2.2.2]octane core (please, see SI, pages 52-54). The commercialized drug Imatinib is used in practice as a mesylate salt. However, to estimate the impact of the replacement of the phenyl ring with bioisosteres on the physicochemical properties, we prepared and studied all three compounds, - **85, 86**, Imatinib, - as free bases.

From amine **87**, in three steps we synthesized compound **88** - a saturated analog of Vorinostat (Fig. 8). For comparison, we also obtained analog **89** with the bicyclo[2.2.2]octane skeleton (please, see SI, pages 56, 57).

Physicochemical properties

Replacement of the *para*-substituted phenyl ring in Imatinib by bicyclo[2.2.2]octane (**86**) decreased the water solubility by more than three times (Fig. 7). However, the incorporation of the 2-oxabicyclo[2.2.2]octane (**85**) in Imatinib increased the solubility close to the original values: 351 μM (Imatinib) vs 113 μM (**86**) vs 389 μM (**85**).

To study the replacement of the phenyl ring with saturated bioisosteres on lipophilicity, we used two characteristics: calculated (clogP)[66] and experimental (logD) lipophilicities. Incorporation of bicyclo[2.2.2]octane in sted of the phenyl ring resulted in a decrease of clogP: 4.5 (Imatinib) vs 3.6 (**86**). The incorporation of 2-oxabicyclo[2.2.2]octane led to an even further decrease of clogP: 2.6 (**85**). A somewhat similar trend was observed with the experimental lipophilicity, logD. While the incorporation of the bicyclo[2.2.2]octane core into Imatinib did not significantly affect it; incorporation of the 2-oxabicyclo[2.2.2]octane core reduced it by ca. one unit, logD: 2.6 (Imatinib) vs 2.7 (**86**) vs 1.8 (**85**).

The effect of saturated bioisosteres on metabolic stability was studied next. The incorporation of both bicyclo[2.2.2]octane (**86**) and 2-oxabicyclo[2.2.2]octane (**85**) into Imatinib, increased the metabolic stability in human liver microsomes: CL_{int} (mg/(min•μL)) = 28 (Imatinib) vs 16 (**86**) vs 19 (**85**) (Fig. 7). Moreover, incorporation of the 2-oxabicyclo[2.2.2]octane core (**85**) into Imatinib increased the life half time by almost 50%: $t_{1/2}$ (min) = 60 (Imatinib) vs 87 (**85**).

In summary, the replacement of the *para*-substituted phenyl ring in Imatinib with common bicyclo[2.2.2]octane core (**86**) led to an undesired three-times decrease in water solubility. At the same time, analogous replacement with 2-oxabicyclo[2.2.2]octane (**85**) resulted in an improvement of all measured physicochemical parameters: increased solubility, enhanced metabolic stability, and reduced lipophilicity.

Biological activity

Finally, to answer a key question, - whether the 2-oxabicyclo[2.2.2]octane core could indeed mimic the phenyl ring in bioactive compounds, we measured the biological activity of Imatinib versus its analogs **85, 86**; and Vorinostat versus its analogs **88, 89**.

We studied the inhibitory effect of Imatinib, Staurosporine, and compounds **85, 86** on the catalytic activity of ABL1 kinase. While the expected activity of Imatinib and Staurosporine was confirmed; we did not observe any significant inhibitory effect of compounds **85, 86** on the ABL1 kinase (please, see SI, pages 294, 295; Supplementary Figs. 13–15). The observed results correlate well with the previous study by Nicolaou, Vourloumis, and Stepan who demonstrated that the replacement of the *para*-substituted phenyl ring in Imatinib with various saturated cyclic cores, including bicyclo[1.1.1]pentane and cubane, led to a dramatic loss of potency against the ABL1 kinase[67].

To study the biological activity of Vorinostat and its analogs **88, 89**, we evaluated their effect on human hepatocellular carcinoma cells HepG2 by fluorescent microscopy (please, see SI, pages 296-300; Supplementary Figs. 16–19). The cells were incubated with the compounds for 48 hours. Staining with specific dyes revealed that all three compounds promoted caspase-dependent cell death, - apoptosis, - that further precipitated in necrosis when the cellular membrane lost its integrity. Vorinostat treatment resulted in 7.2% and 12.2% of apoptotic cells upon incubation at concentrations 5 μM and 50 μM respectively (Fig. 9). Analogs **88** and **89** demonstrated similar efficacy only at 50 μM.

These primary biological results (Fig. 9) suggested that Vorinostat and both its analogs **88, 89** could have similar cytotoxic and cytostatic

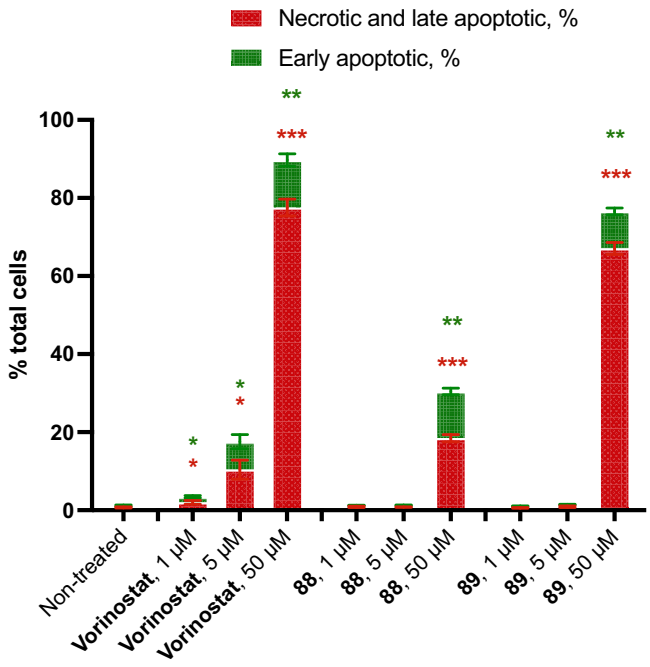

Fig. 9 | Anticancer activity of Vorinostat (SAHA) and its saturated analogs 88, 89. Types of HepG2 cell death (% of total cells) after treatment with *Vorinostat* and compounds **88, 89** (1 μM, 5 μM, and 50 μM) for 48 h. Red: necrotic cell death. Green: early apoptotic cell death. The data were presented as mean ± SEM ($n = 3$, independent wells for every of which approx. 2000 visualized cells were analyzed).* - indicates $P < 0.05$, ** - indicates $P < 0.01$, *** - $P < 0.001$ compared with the non-treated group in a two-tailed unpaired t-test with Welch correction on each row of data.

activities in cells (for a more comprehensive comparison of Vorinostat and its analogs **88**, **89**, additional experiments on the enzyme potency and selectivity are needed).

Virtual libraries

To analyze how the replacement of the *para*-substitued phenyl ring with 2-oxabicyclo[2.2.2]octane affects 3D-shape of organic compounds, we generated two virtual libraries based on *C*- and *N*-terminus modifications of *para*-aminobenzoic acid and its 2-oxabicyclo[2.2.2] octane-containing analog. Each library contained 5000 molecules (Supplementary Data 6, Supplementary Data 7). According to principal moments of inertia (PMI) plots, both libraries occupied essentially the same region in 3D-chemical space. The same was true for FDA-approved drugs Aminopterin, Conivaptan, Deferasifox, Tetracaine, and their 2-oxabicyclo[2.2.2]octane-containing analogs (for details, please see SI, pages 301–304; Supplementary Table 8, Supplementary Figs. 20 and 21).

In conclusion, we have designed, synthesized, and characterized a new saturated bioisostere of the phenyl ring - 2-oxabicyclo[2.2.2] octane. In the design of the structure, we kept all advantages of the previously used cores (bicyclo[1.1.1]pentane, bicyclo[2.2.2]octane, cubane): conformational rigidity, metabolic stability, non-chirality, and collinearity of the exit vectors (Fig. 1c). In addition, we addressed their disadvantages: C-C distance and lipophilicity (Fig. 1c). Thus the 2-oxabicyclo[2.2.2]octane scaffold designed here was synthesized from available starting materials on a multigram scale (Table 1) - up to 135 g in one run (Fig. 2). The key synthesis step was the iodocyclization of cyclohexane-containing alkenyl alcohols with molecular iodine in acetonitrile (Figs. 2 and 3). Crystallographic analysis revealed its high similarity with the *para*-substituted phenyl ring (Fig. 5). 2-Oxabicyclo[2.2.2]octane core was incorporated into the structure of Imatinib and Vorinostat drugs instead of the *para*-substituted and the *mono*-substituted phenyl rings, correspondingly (Figs. 7 and 8). In the case of Imatinib, the formed saturated analog **85** possessed improved physicochemical properties over the drug: increased water solubility, enhanced metabolic stability, and reduced lipophilicity (Fig. 7). In the case of Vorinostat (SAHA), the formed saturated analog **88** exhibited a similar biological activity compared to that of the drug (Fig. 9).

This study enhances the repertoire of available saturated bioisosteres of (hetero)aromatic rings for use in drug discovery projects.

Methods

General procedure for the iodocyclization

To a solution of alkene **5** (222.64 g, 1.21 mol, 1.00 equiv) in MeCN (4000 mL) were added $NaHCO_3$ (243.94 g, 2.90 mol, 2.40 equiv) in one portion and I_2 (736.60 g, 2.90 mol, 2.40 equiv) in four portions. The resulting mixture was stirred for 12 h at room temperature. Then sodium thiosulfate pentahydrate (900.24 g, 3.63 mol, 3.00 equiv) and distilled water (2000 mL) were added to the mixture. The colorless mixture was extracted with MeO*t*Bu (10 × 400 mL). The combined organic layers were concentrated under reduced pressure to dryness. The residue was dissolved in MeO*t*Bu (1000 mL), washed with brine (1 × 400 mL), a saturated solution of $Na_2S_2O_3$ (3 × 400 mL), dried over Na_2SO_4, filtered through a plug of SiO_2 (0.5 L glass filter filed with 3 cm in high with silica gel) and concentrated. The final product was purified by column chromatography (SiO_2, hexane:EtOAc = 1:5, $R_f = 0.7$) to provide pure iodide **6**. Yield: 135.16 g, 0.436 mol, 36%, white solid.

NMR spectra were analyzed with MestreNova (11.0.3-18688).

Reporting summary

Further information on research design is available in the Nature Portfolio Reporting Summary linked to this article.

Data availability

Experimental data as well as characterization data for all new compounds prepared during these studies are provided in the Supplementary Information of this manuscript. The X-ray crystallographic coordinates for compounds **30**, **57**, **67**, **69**, and **78** have been deposited at the Cambridge Crystallographic Data Centre (CCDC) with accession codes 2226162 (**30**), 2226164 (**57**), 2226872 (**67**), 2226163 (**69**), 2266656 (**78**). These data can be obtained free of charge from the Cambridge Crystallographic Data Centre via www.ccdc.cam.ac.uk/structures/. A source data file is available for the biological activity of Imatinib with analogs **85**, **86**; and Vorinostat with analogs **88**, **89**. Source data are provided with this paper.

References

1. Chen, Y., Rosenkranz, C., Hirte, S. & Kirchmair, J. Ring systems in natural products: structural diversity, physicochemical properties, and coverage by synthetic compounds. *Nat. Prod. Rep.* **39**, 1544–1556 (2022).
2. Taylor, R. D., MacCoss, M. & Lawson, A. D. G. Rings in drugs. *J. Med. Chem.* **57**, 5845–5859 (2014).
3. Shearer, J., Castro, J. L., Lawson, A. D. G., MacCoss, M. & Taylor, R. D. Rings in clinical trials and drugs: present and future. *J. Med. Chem.* **65**, 8699–8712 (2022).
4. The search was performed at https://go.drugbank.com on 05 July 2023.
5. Ritchie, T. J. & Macdonald, S. J. F. The impact of aromatic ring count on compound developability – are too many aromatic rings a liability in drug design? *Drug Discov. Today* **14**, 1011–1020 (2009).
6. Lovering, F., Bikker, J. & Humblet, C. Escape from Flatland: increasing saturation as an approach to improving clinical success. *J. Med. Chem.* **52**, 6752–6756 (2009).
7. Lovering, F. Escape from Flatland 2: complexity and promiscuity. *Med. Chem. Commun.* **4**, 515–519 (2013).

8. Stepan, A. F. et al. Application of the bicyclo[1.1.1]pentane motif as a nonclassical phenyl ring bioisostere in the design of a potent and orally active γ-secretase inhibitor. *J. Med. Chem.* **55**, 3414–3424 (2012).
9. Measom, N. D. et al. Investigation of a bicyclo[1.1.1]pentane as a phenyl replacement within an $LpPLA_2$ inhibitor. *ACS Med. Chem. Lett.* **8**, 43–48 (2017).
10. Goh, Y. L., Cui, Y. T., Pendharkar, V. & Adsool, V. A. Toward resolving the resveratrol conundrum: synthesis and in vivo pharmacokinetic evaluation of BCP–resveratrol. *ACS Med. Chem. Lett.* **8**, 516–520 (2017).
11. Pu, Q. et al. Discovery of potent and orally available bicyclo[1.1.1] pentane-derived indoleamine-2,3-dioxygenase 1 (IDO1) inhibitors. *ACS Med. Chem. Lett.* **11**, 1548–1554 (2020).
12. Chalmers, B. A. et al. Validating eaton's hypothesis: cubane as a benzene bioisostere. *Angew. Chem. Int. Ed.* **55**, 3580–3585 (2016).
13. Wiesenfeldt, M. P. et al. General access to cubanes as benzene bioisosteres. *Nature* **618**, 513–518 (2023).
14. Reekie, T. A., Williams, C. M., Rendina, L. M. & Kassiou, M. Cubanes in medicinal chemistry. *J. Med. Chem.* **62**, 1078–1095 (2019).
15. Bernhard, S. S. R. et al. Cross-coupling and cubane–porphyrin arrays. *Chem. Eur. J.* **24**, 1026–1030 (2018).
16. Houston, S. D. et al. The cubane paradigm in bioactive molecule discovery: further scope, limitations and the cyclooctatetraene complement. *Org. Biomol. Chem.* **17**, 6790–6798 (2019).
17. Flanagan, K. J., Bernhard, S. S. R., Plunkett, S. & Senge, M. O. Not your usual bioisostere: solid state study of 3d interactions in cubanes. *Chem. Eur. J.* **25**, 6941–6954 (2019).
18. Wlochal, J., Davies, R. D. M. & Burton, J. Cubanes in medicinal chemistry: synthesis of functionalized building blocks. *Org. Lett.* **16**, 4094–4097 (2014).
19. Dallaston, M. A., Brusnahan, J. S., Wall, C. & Williams, C. M. Thermal and sensitiveness determination of cubanes: towards cubane-based fuels for infrared countermeasures. *Chem. Eur. J.* **25**, 8344–8352 (2019).
20. Zhong, M. et al. Discovery of functionalized bisimidazoles bearing cyclic aliphatic-phenyl motifs as HCV NS5A inhibitors. *Bioorg. Med. Chem. Lett.* **24**, 5731–5737 (2014).
21. Bandak, D., Babii, O., Vasiuta, R., Komarov, I. V. & Mykhailiuk, P. K. Design and synthesis of novel ^{19}F-amino acid: a promising ^{19}F NMR label for peptide studies. *Org. Lett.* **17**, 226–229 (2015).
22. Aguilar, A. et al. Discovery of 4-((3′R,4′S,5′R)-6″-Chloro-4′-(3-chloro-2-fluorophenyl)-1′-ethyl-2″-oxodispiro[cyclohexane-1,2′-pyrrolidine-3′,3″-indoline]-5′-carboxamido)bicyclo[2.2.2]octane-1-carboxylic Acid (AA-115/APG-115): a potent and orally active murine double minute 2 (MDM2) inhibitor in clinical development. *J. Med. Chem.* **60**, 2819–2839 (2017).
23. Mykhailiuk, P. K. Saturated bioisosteres of benzene: where to go next? *Org. Biomol. Chem.* **17**, 2839–2849 (2019).
24. Locke, G. M., Bernhard, S. S. R. & Senge, M. O. Nonconjugated hydrocarbons as rigid-linear motifs: isosteres for material sciences and bioorganic and medicinal chemistry. *Chem. Eur. J.* **25**, 4590–4647 (2019).
25. Subbaiah, M. A. M. & Meanwell, N. A. Bioisosteres of the phenyl ring: recent strategic applications in lead optimization and drug design. *J. Med. Chem.* **64**, 14046–14128 (2021).
26. Zhao, J.-X. et al. 1,2-Difunctionalized bicyclo[1.1.1]pentanes: Long–sought-after mimetics for ortho/meta-substituted arenes. *PNAS* **18**, e2108881118 (2020). Replacement of the *ortho*- and *meta*-substituted phenyl rings in bioactive compounds with saturated bioisosteres was also recently achieved (Refs 26-31).
27. Denisenko, A., Garbuz, P., Shishkina, S. V., Voloshchuk, N. M. & Mykhailiuk, P. K. Saturated bioisosteres of *ortho*-substituted benzenes. *Angew. Chem. Int. Ed.* **59**, 20515–20521 (2020).
28. Frank, N. et al. Synthesis of *meta*-substituted arene bioisosteres from [3.1.1]propellane. *Nature* **611**, 721–726 (2022).
29. Epplin, R. C. et al. [2]-Ladderanes as isosteres for meta-substituted aromatic rings and rigidified cyclohexanes. *Nat. Commun.* **13**, 6056 (2022).
30. Denisenko, A. et al. 2-Oxabicyclo[2.1.1]hexanes as saturated bioisosteres of the ortho-substituted phenyl ring. *Nat. Chem.* **15**, 1155–1163 (2023).
31. Dibchak, D. et al. General synthesis of 3-azabicyclo[3.1.1]heptanes and evaluation of their properties as saturated isosteres. *Angew. Chem. Int. Ed.* e202304246 (2023).
32. Kanazawa, J. & Uchiyama, M. Recent advances in the synthetic chemistry of bicyclo[1.1.1]pentane. *Synlett* **30**, 1–11 (2019).
33. Ma, X. & Pham, L. N. Selected topics in the syntheses of bicyclo[1.1.1] pentane (BCP) analogues. *Asian J. Org. Chem.* **9**, 8–22 (2020).
34. Gianatassio, R. et al. Strain release amination. *Science* **351**, 241–246 (2016).
35. Caputo, D. F. J. et al. Synthesis and applications of highly functionalized 1-halo-3-substituted bicyclo[1.1.1]pentanes. *Chem. Sci.* **9**, 5295–5390 (2018).
36. Pickford, H. D. et al. Twofold radical-based synthesis of N,C-difunctionalized bicyclo[1.1.1]pentanes. *J. Am. Chem. Soc.* **143**, 9729–9736 (2021).
37. Bychek, R. & Mykhailiuk, P. K. A practical and scalable approach to fluoro-substituted bicyclo[1.1.1]pentanes. *Angew. Chem. Int. Ed.* **61**, e202205103 (2022).
38. Pickford, H. D. et al. Rapid and scalable halosulfonylation of strain-release reagents. *Angew. Chem. Int. Ed.* **62**, e202213508 (2023).
39. Ripenko, V., Vysochyn, D., Klymov, I., Zhersh, S. & Mykhailiuk, P. K. Large-scale synthesis and modifications of bicyclo[1.1.1]pentane-1,3-dicarboxylic acid (BCP). *J. Org. Chem.* **86**, 14061–14068 (2021).
40. Bychek, R. M. et al. Difluoro-substituted bicyclo[1.1.1]pentanes for medicinal chemistry: design, synthesis, and characterization. *J. Org. Chem.* **84**, 15106–15117 (2019).
41. Auberson, Y. P. et al. Improving non-specific binding and solubility: bicycloalkyls and cubanes as p-phenyl bioisosteres. *ChemMedChem* **12**, 590–598 (2017).
42. Houston, S. D. et al. Cyclooctatetraenes through valence isomerization of cubanes: scope and limitations. *Chem. Eur. J.* **25**, 2735–2739 (2019).
43. Takebe, H. & Matsubara, S. Catalytic asymmetric synthesis of 2,6-disubstituted cuneanes through enantioselective constitutional isomerization of 1,4-disubstituted cubanes. *Eur. J. Org. Chem.* **37**, e202200567 (2022).
44. Wang, L. et al. Mechanochemistry of cubane. *J. Am. Chem. Soc.* **144**, 22865–22869 (2022).
45. Toriyama, F. et al. Redox-active esters in Fe-catalyzed C–C coupling. *J. Am. Chem. Soc.* **138**, 11132–11135 (2016).
46. He, J. et al. Ligand-promoted borylation of $C(sp^3)$-H bonds with palladium(II). *Catalysts. Angew. Chem. Int. Ed.* **55**, 785–789 (2016).
47. Hanson, A. M. et al. A–C estrogens as potent and selective estrogen receptor-beta agonists (SERBAs) to enhance memory consolidation under low-estrogen conditions. *J. Med. Chem.* **61**, 4720–4738 (2018).
48. Shaw, S. A. et al. Discovery and structure activity relationships of 7-benzyl triazolopyridines as stable, selective, and reversible inhibitors of myeloperoxidase. *Bioorg. Med. Chem.* **28**, 115723 (2020).
49. Koko, M., Anderluh, M., Hrast, M. & Minovski, N. The structural features of novel bacterial topoisomerase inhibitors that define their activity on topoisomerase IV. *J. Med. Chem.* **65**, 6431–6440 (2022).
50. Singh, S. B. et al. Oxabicyclooctane-linked novel bacterial topoisomerase inhibitors as broad spectrum antibacterial agents. *ACS Med. Chem. Lett.* **5**, 609–614 (2014).

51. Singh, S. B. et al. Structure activity relationship of C-2 ether substituted 1,5-naphthyridine analogs of oxabicyclooctane-linked novel bacterial topoisomerase inhibitors as broad-spectrum antibacterial agents (Part-5). *Bioorg. Med. Chem. Lett.* **25**, 3630–3635 (2015).
52. Singh, S. B. et al. C1–C2-linker substituted 1,5-naphthyridine analogues of oxabicyclooctane-linked NBTIs as broad-spectrum antibacterial agents (part 7). *Med. Chem. Commun.* **6**, 1773–1780 (2015).
53. Tan, C. M. et al. In vitro and in vivo characterization of the novel oxabicyclooctane-linked bacterial topoisomerase inhibitor AM-8722, a selective, potent inhibitor of bacterial DNA gyrase. *Antimicrob. Agents Chemother.* **22**, 4830–4839 (2016).
54. Harrison, T. J. et al. Successful strategies for mitigation of a preclinical signal for phototoxicity in a DGAT1 inhibitor. *ACS Med. Chem. Lett.* **10**, 1128–1133 (2019).
55. Lu, Z. et al. Identification of potent, selective and orally bioavailable phenyl ((*R*)-3-phenylpyrrolidin-3-yl)sulfone analogues as RORγt inverse agonists. *Bioorg. Med. Chem. Lett.* **29**, 2265–2269 (2019).
56. Levterov, V. V., Panasyuk, Y., Pivnytska, V. O. & Mykhailiuk, P. K. Water-soluble non-classical benzene mimetics. *Angew. Chem. Int. Ed.* **59**, 7161–7167 (2020).
57. Kraus, G. A. & Thurston, J. Alkoxy radicals in organic synthesis. A novel approach to spiroketals. *Tetrahedron Lett.* **28**, 4011–4014 (1987).
58. Qin, T. et al. Nickel-catalyzed barton decarboxylation and giese reactions: a practical take on classic transforms. *Angew. Chem. Int. Ed.* **56**, 260–265 (2017).
59. Yang, Y. et al. Practical and modular construction of C(sp^3)-rich alkyl boron compounds. *J. Am. Chem. Soc.* **143**, 471–480 (2021).
60. Wang, J. et al. Cu-catalyzed decarboxylative borylation. *ACS Catal.* **8**, 9537–9542 (2018).
61. Yao, S. et al. Photoredox-promoted alkyl radical addition/semi-pinacol rearrangement sequences of alkenylcyclobutanols: rapid access to cyclic ketones. *Chem. Commun.* **54**, 8096–8099 (2018).
62. Urner, L. M. et al. Systematic variation of cyanobuta-1,3-dienes and expanded tetracyanoquinodimethane analogues as electron acceptors in photoactive, rigid porphyrin conjugates. *Eur. J. Org. Chem.* **2015**, 91–108 (2015).
63. Bloomfield, A. J., Chaudhuri, S., Mercado, B. Q., Batista, V. S. & Crabtree, R. H. Facile solvolysis of a surprisingly twisted tertiary amide. *N. J. Chem.* **40**, 1974–1981 (2016).
64. Nagar, B. et al. Crystal structures of the kinase domain of c-Abl in complex with the small molecule inhibitors PD173955 and Imatinib (STI-571). *Cancer Res.* **62**, 4236–4243 (2002).
65. Doerwald, F. Z. *Lead optimizations for medicinal chemists* (Wiley-VCH, 2012).
66. *clogP was calculated with "Cxcalc"* (ChemAxon, version 22.5.0) (2022).
67. Nicolaou, K. C. et al. Synthesis and biopharmaceutical evaluation of imatinib analogues featuring unusual structural motifs. *ChemMedChem* **11**, 31–37 (2016).

Acknowledgements

The authors are grateful to Prof. A. A. Tolmachev for the support of this work. This project has received funding from the European Research Council (ERC) under the European Union's Horizon 2020 research and innovation program (grant agreement No. 101000893 - BENOVELTY). P.K.M. is very grateful to Dr. S. Shishkina (IOC, Kyiv) for the X-ray studies, to Dr. D. Bylina for HRMS measurements, to K. Fominova and V. Kokhalskiy for the help with the synthesis of compounds **35** and **39**, and to Dr. V. Kubyshkin for proofreading the manuscript.

Author contributions

V.V.L., I.S., P.B., and P.K.M. designed the experiments. V.V.L., Y.P., K.S., O.S., V.B., O.S., I.S., L.B., O. K.-U., Y.H., L.L., P.B., K.H., I.B., J.P.B., D.D. conducted and analyzed the experiments described in this report. P.B. and P.K.M. prepared this manuscript for publication.

Competing interests

The authors declare the following competing interests: V.V.L., Y.P., K.S., O.S., V.B., O.S., I.S., L.B., O.K.-U., Y.H., P.B., K.H., I.B., D.D., P.K.M. are employees of a chemical supplier Enamine. The remaining authors declare no competing interests.

Additional information

Supplementary information The online version contains supplementary material available at https://doi.org/10.1038/s41467-023-41298-3.

Correspondence and requests for materials should be addressed to Pavel K. Mykhailiuk.

Peer review information *Nature Communications* thanks Edward Anderson, Bin Yu and the other, anonymous, reviewer(s) for their contribution to the peer review of this work. A peer review file is available.